INTERNATIONAL JOURNAL OF REFRIGERATION 50 (2015) 69–79

Available online at www.sciencedirect.com

ScienceDirect

journal homepage: www.elsevier.com/locate/ijrefrig

Fault and sensor error diagnostic strategies for a vapor compression refrigeration system by using fuzzy inference systems and artificial neural network

Necati Kocyigit *

Dept. of Energy Systems Engineering, Recep Tayyip Erdogan University, 53100 Rize, Turkey

ARTICLE INFO

Article history:
Received 24 June 2014
Received in revised form
12 October 2014
Accepted 18 October 2014
Available online 27 October 2014

Keywords:
Vapor refrigeration
Faults and errors diagnosis
Fuzzy inference system
Artificial neural network

ABSTRACT

A fuzzy inference system (FIS) and an artificial neural network (ANN) were used for diagnosis of the faults of a vapor compression refrigeration experimental setup. A separate FIS was developed for detection of sensor errors. The fault estimation error of the FIS and ANN were evaluated by using the experimentally obtained sensor data. Separate FIS estimated the system faults and detected defective sensors in all test cases without any error. Levenberg Marquart (LM) type ANN algorithm was implemented to diagnose the system faults. Scaled conjugate gradient (SCG) and resilient backpropagation (RB) network type were also used to compare performances with the estimation of the LM algorithm. The LM type ANN estimated all fault conditions accurately in the test cases never observed before. The study demonstrated that the FIS and ANN could be used effectively to estimate the faulty conditions of the vapor compression refrigeration system.

© 2014 Elsevier Ltd and IIR. All rights reserved.

Stratégies de diagnostic des défaillances et des erreurs de captation dans un système frigorifique à compression de vapeur utilisant des stratégies d'inférence floues et un réseau neuronal artificiel

Mots clés : Froid par vapeur ; Diagnostic des fautes et erreurs ; Système d'inférence floue ; Réseau neuronal artificiel

1. Introduction

Heating, ventilation, air conditioning, and refrigeration (HVAC&R) systems operated under faulty conditions often result in extra energy consumptions of up to 30% for commercial buildings, when multiple faults happening simultaneously (Han et al., 2011). Faults in vapor compression system have led to increase chiller energy consumption and decrease

* Tel.: +90 5308823740; fax: +90 4642280025.
E-mail addresses: dr.necati.kocyigit@gmail.com, necati.kocyigit@erdogan.edu.tr.
http://dx.doi.org/10.1016/j.ijrefrig.2014.10.017
0140-7007/© 2014 Elsevier Ltd and IIR. All rights reserved.

Nomenclature

$\dot{m}$	mass flow rate (kg s^{-1})
P	pressure (kPa)
p-h	pressure-enthalpy
R	error
T	temperature (°C)
μ	membership degree

Abbreviation

ANN	artificial neural network
AXV	automatic expansion valve
ARX	exogenous variables
EEV	electrical expansion valve
FDD	fault detection and diagnosis
FDFIS	fault diagnostic fuzzy inference system
FIS	fuzzy inference system
HVAC&R	heating, ventilating, air conditioning & refrigeration
SDFIS	sensor diagnostic fuzzy inference system
TXV	thermostatic expansion valve
H	high
HP	high pressure
HP-M	high pressure sensor error
L	low
LP	low pressure
LP-M	low pressure sensor error
Mref	mass flow rate of refrigerant
Mref-M	mass flow rate sensor error
N	normal
No	no differences
VL	very low
PH	partially high
PL	partially low
SV	solenoid valve
SC	subcooling
SC-M	subcooling sensor error
SH	superheat
SH-M	superheat sensor error
Tsur	surface temperature of compressor
Tsur-M	surface temperature sensor
VH	very high

Subscripts

a	air
ave	average
c	condenser
comp	compressor
dis	discharge
e	evaporator
LP	low pressure
max	maximum values
min	minimum values
ref	refrigerant
sat	saturated
suc	suction
sur	surface of compressor
sc	subcooling
sh	superheat

chiller efficiency (Zhao et al., 2012). Because cooling and refrigeration cause over a third of the electrical energy consumption in residential and commercial buildings, detecting incipient faults leads to reduce the energy cost and save the energy consumption. Reducing the energy consumption is significant for the environment as well.

In the late 1980s, the earlier development of diagnostics systems for HVAC&R systems was mainly implemented by rule-based expert systems. During the late 1990s, the development of automating fault detection and diagnosis was given emphasis. Inputs and outputs of the HVAC&R operating process are to be mathematically related to each other by using autoregressive models with exogenous variables (ARX), artificial neural network (ANN) models, and numerous other developing models (Wang, 2001). Both ARX and ANN are named as black-box because they have need of less physical knowledge of the operating process.

In general, present fault detection and diagnosis (FDD) algorithms for vapor compression cycles have two categories: steady-state model-based algorithms and neural network/fuzzy model approaches (Halm-Owoo and Suen, 2002). In the recent years, many researchers have carried out numerous studies on the vapor compression system faults. A data mining method and an ANN were combined to detect and diagnosis sensor faults in HVAC systems (Hou et al., 2006). All FDD features in the steady-state detector were imposed by using seven measurements in a vapor compression system (Kim et al., 2008). A reference model to predict the value of system parameters during fault-free operation for fault detection and diagnosis in a heat pump system was developed by using an ANN (Kim et al., 2010). A split residential heat pump with a thermostatic expansion valve (TXV) was tested during steady-state no-fault and imposed-fault operation. Faults such as compressor valve leakage, outdoor improper air flow, indoor improper air flow, liquid line restriction, refrigerant undercharge, and refrigerant overcharge were imposed. Evaporator fouling, condenser fouling, and refrigerant overcharge have led to cause the greatest performance degradation (Yoon et al., 2011). A hybrid method incorporating auto-regressive model with ARX and support vector machines (SVM) were imposed for FDD in chillers (Yan et al., 2014). A decoupling-based FDD method with multiple simultaneous faults was fully implemented online and evaluated in the field test environment. (Zhao et al., 2014). Other related publications of research on FDD have also been presented (Bulgurcu, 2009; Piacentino and Talamo, 2013). The author recently detected eight faulty conditions in a vapor compression refrigeration system with hermetic reciprocating compressor by using the refrigeration cycle on the p-h diagram (Kocyigit et al., 2014).

Furthermore, sensor error methods were applied to several systems in the recent years. A method (virtual fouling monitor sensor) using chiller measurement for monitoring the fouling status of the condenser was imposed to detect the condenser fouling faults in chillers. The proposed virtual fouling monitor sensor was also implemented and evaluated on a field chiller (Zhao et al., 2012). A new fault diagnosis method for sensors in an air-handling unit based on neural network pre-processed by wavelet and fractal was imposed. By comparing the

Table 1 – Fault codes, fault modes, description of faults, and determination of level of fault.

Fault codes	Fault Modes	Descriptions of faults	Determination of level of fault during test
0	NC	Normal condition	fault free test
1	CDW	Compressor failure-doesn't work	compressor switch off
2	RFD	Restricted filter-drier	% of normal pressure drop through AXV
3	RXV	Restricted automatic expansion valve	% of normal pressure drop through evaporator
4	CVL	Compressor valve leakage	% of refrigerant flow rate
5	RU	Refrigerant undercharge	% undercharge from the correct charge
6	RO	Refrigerant overcharge	% overcharge from the correct charge
7	DC	Dirty condenser	% of air flow rate reduction
8	EFF	Evaporator fan failure	evaporator fan switch off

prediction with the objective vectors, the sensor faults could be diagnosed (Zhu et al., 2012).

In this study, a new fault diagnostic method was proposed to diagnose the system faults of a vapor compression refrigeration system with the hermetic reciprocating compressor. The proposed diagnostic method was diagnosed the system faults by using fuzzy inference system (FIS) and ANN.

Moreover, an error diagnostic method was proposed to detect the sensor error by using FIS. The proposed methods were based on FIS that emphasized how to diagnose the system faults and to detect the errors of the sensors by using the sensor data of the refrigeration system.

Furthermore, ANN was also used for the diagnosis of the system faults. The proposed approaches had much more diagnostic ability to diagnose automatically the system faults and detect the sensor errors.

2. Theoretical background

A Fuzzy Inference System (FIS) maps an input space to an output space using fuzzy logic. FIS uses a collection of fuzzy membership functions and rules, instead of crisp logic, to classify the data. A membership function (MF) gives a degree of membership having between 0 and 1 to a variable in a fuzzy set. The behavior of FIS is characterized by a set of linguistic rules which establishes a rule base (Abraham, 2005).

In this study, a standard Mamdani fuzzy inference system was used to compute the outputs of FIS for the given inputs. In the Mamdani-type fuzzy system, the if-then rules comprise linguistic variables associated with fuzzy concepts. A linguistic fuzzy-rule base consists of the expression of the form (Abraham, 2005):

$$\text{If a then b} \tag{1}$$

where a and b are fuzzy statements.

Mamdani FIS must go through six steps: i) establish a set of fuzzy rules, ii) fuzzifying the given cases by using the membership functions by the user, iii) calculation of the rule strength by combining the fuzzified cases according to the fuzzy rules, iv) determining the output membership function from the rule strength and the output membership function, v) to obtain the output distribution based on the consequences to get an output distribution, and vi) defuzzifying the determined output distribution (Abraham, 2005).

ANNs can be used for either prediction or classification problems. ANNs, inspired by biological neurons, comprise massively interconnected nodes named as neurons. These neurons are linked together to form a network architecture. ANNs use multiple layers which has multiple hidden nodes. These layers are named as input, hidden, and output layer. These layers consist of input nodes, hidden nodes, and output nodes, respectively. The information involved in the input layer is mapped to the output layer through the hidden layer(s). Each neuron can send its output to the neurons only on the higher layer and receive its input from the lower layer (Ertunc and Hosoz, 2008).

In this study, three types of ANN algorithm were employed to diagnose the system faults. The Levenberg–Marquardt (LM) algorithm (Kizilkan, 2011), Scaled conjugate gradient backpropagation (SCG) (Kizilkan, 2011), and Resilient Backpropagation (RB) (Mavromatidis et al., 2013) were used to model the considered system.

3. Previous fault detection study of the author

The p-h diagram of the refrigeration cycle was used for the diagnosis of the vapor compression refrigeration system by following the similar implementation in our previous study (Kocyigit et al., 2014). The variables of the thermodynamic properties were monitored for detection of the faults. Eight faulty and one normal condition were assigned to variables for diagnosis of the vapor compression refrigeration system. They were named as shown in Table 1 (Kocyigit et al., 2014).

Each fault mode was explained respectively as below:

1) CDW: When the compressor does not work, both of the low side (LP) and high side pressures (HP) have the same value.
2) RFD: If the filter-drier is restricted or clogged, its surface will get cold. Both the low side and high side pressures decrease and the superheat as well as the subcooling increase. Because of the additional expansion in the liquid line, the refrigerant mass flow reduces, thereby decreasing the refrigeration capacity.
3) RXV: If the automatic expansion valve is restricted or partially clogged, its surface will frost. In this case, both of the low side and high side pressures decrease, and the degrees of the suction superheat and the subcooling increase. Because of a restricted refrigerant flow, the refrigerant mass flow rate reduces, thereby decreasing the refrigeration capacity.

4) CVL: Compressor valve leakage can be done because of worn cylinder surfaces and piston rings as well as clogged valve plate. Thus, the refrigerant mass flow rate decreases in the refrigeration system. The low side pressure increases and the high side pressure decreases, while the degrees of the suction superheat and the subcooling increase. The refrigerant mass flow rate reduces, thus decreasing the refrigeration capacity.
5) RU: This type failure can be simulated by transferring the liquid refrigerant to the accumulator. As the refrigerant charge of system decreases, both the low and high side pressures decrease, the degrees of the suction superheat increases while the subcooling decreases. The refrigerant mass flow rate reduces, thus decreasing the refrigeration capacity.
6) RO: If the refrigerant is transferred to the system from accumulator, this type of failure can be simulated. As the refrigerant charge of system increases, both the evaporator and condenser pressures increase and degrees of the suction superheat and the subcooling decrease. The refrigerant mass flow rate increases, thereby increasing the refrigeration capacity.
7) DC: When the condenser is clogged by leafs, paper pieces, dust, etc., the heat transfer capacity of the condenser reduces. Eighty percent of fault levels are implemented by blocking the corresponding percentage of the finned frontal area of the condenser. In this failure case, the degree of the subcooling decreases but the suction superheat increases.
8) EFF: If the evaporator fan motor does not work, the heat transfer coefficient decreases in the evaporator. The refrigerant does not evaporate in the evaporator, and then it flows through the suction line to the compressor in the liquid phase. This condition is very detrimental for the compressor. The low side and high side pressures decrease, the degree of the suction superheat is very low, but subcooling increases. The low pressure switch opens the control circuit. The refrigeration capacity decreases because of the ice layer and shorted cycle.

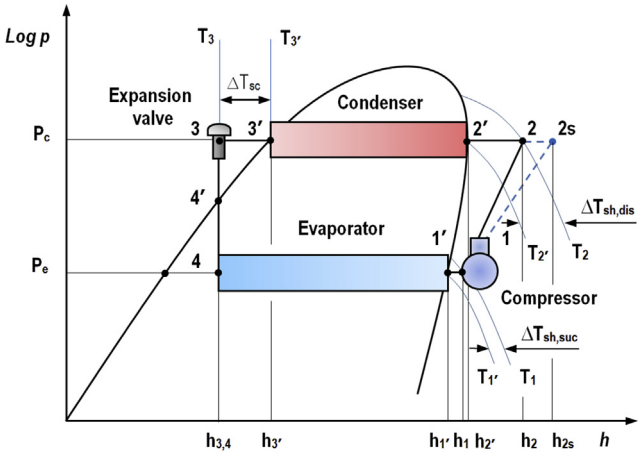

Fig. 1 – Points of meaningful instrument readings in refrigeration cycle on the p-h diagram. (P_c: Condenser pressure, P_e: Evaporator pressure, h_1: Enthalpy of point 1, $h_{1'}$: Enthalpy of point 1′, h_2: Enthalpy of point 2, $h_{2'}$: Enthalpy of point 2′, h_{2s}: Enthalpy of point 2s, $h_{3,4}$: Enthalpy of point 3 and 4, $h_{3'}$: Enthalpy of point 3′, T_1: Temperature of point 1, $T_{1'}$: Temperature of point 1′, T_2: Temperature of point 2, $T_{2'}$: Temperature of point 2′, T_3: Temperature of point 3, $T_{3'}$: Temperature of point 3′, $\Delta T_{sh,suc}$: Suction superheat, $\Delta T_{sh,dis}$: Discharge superheat, ΔT_{sc}: Subcooling, point 1: Suction, point 1': Saturated vapor point of point 1, point 2: Discharge with constant entropy, point 2s: Discharge with entropy increase, point 2′: Saturated vapor point of point 2, point 3': Saturated liquid of point 3, point 3: Sub-cooled liquid at the expansion valve, point 4': Saturated liquid of point 4, and point 4: Evaporator input).

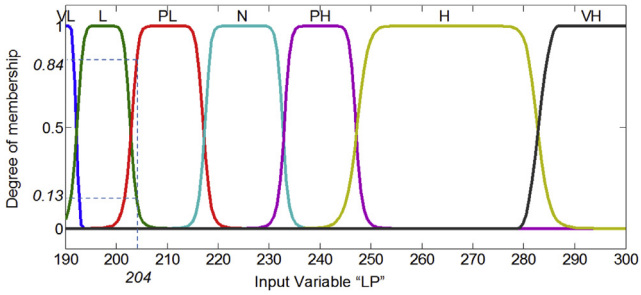

Fig. 2 – Plot out of LP of degree of membership. (VL: Very low, L: Low, N: Normal, PH: Partial high, H: High, VH: Very high, LP: Input variable of low pressure).

The FIS can be used for the fault diagnostics of the refrigeration system from the sensor data. Eight faulty system scenarios were considered. The superheat and subcooling values were calculated from the data of two sensors. Thus, each operating condition had a unique six parameters. In the same way, sensor errors were also detected and the faulty sensor was identified from the data.

ANN was used for prediction of the fault condition when it was trained to identify the fault. ANN was trained by using the input and output data sets. Thus, eight faulty and one normal condition scenarios were used to train the ANN.

4. Proposed fault diagnostic method

In this section, the implementation of the FIS and ANN for the fault diagnosis will be explained first. Then, detection of the sensor errors will be discussed. Some measured and calculated data indicated on the p-h diagram (Fig. 1) was used for evaluating the performance of the fuzzy inference system and the artificial neural network. The measured data was as follows: low side pressure (P_e), high side pressure (P_c), suction temperature of the compressor (T_1), input temperature of the expansion device (T_3), refrigerant mass flow rate ($\dot{m}_{ref}$), and compressor surface temperature (T_{sur}). The calculated data was as follows: the degree of suction superheat (T_{sh}) and the degree of subcooling (T_{sc}).

Furthermore, isentropic efficiency (η_s) had to be calculated for plotting the refrigeration cycle on the p-h diagram.

$$\eta_s = \frac{h_{2s} - h_1}{h_2 - h_1} \quad (2)$$

where h_1, h_{2s}, and h_2 are the enthalpy of the refrigerant at the inlet of the compressor, the enthalpy at the outlet of the compressor for the isentropic compression process, and the enthalpy at the outlet of the compressor for the actual compression process, respectively.

In this study, FIS and ANN methods were implemented for the estimation of the refrigeration system faults and sensor errors. The FIS and ANN were used separately for the estimation of the faults. The FIS was used for detection of sensor errors.

Fuzzy inference system (FIS) and artificial neural networks (ANNs) are good choices for classification of the faults. The FIS and the ANN had ability to estimate the system fault or the sensor error by using the sensor data.

The proposed fault diagnostic FIS for the system faults (FDFIS) had six input membership functions (MFs) and two output MFs, as shown respectively in Fig. 2. The FDFIS held seventeen rules of inference that were used in reasoning.

If the FDFIS detected the unknown status (UNKNOWN), one or more sensors had problems such as a bad connection or broken sensor. The proposed sensor error diagnostic FIS (SDFIS) was developed to detect the sensor errors. In this study, the errors of one or two of six sensors were considered. According to eight faulty and one normal condition scenarios, each faulty and one normal condition had the unique data set. Whenever the system had a faulty condition, the faulty condition was likely diagnosed by using the FDFIS. Otherwise The FDFIS was not able to diagnose the faulty condition due to the error of one or two sensors. In this case, the errors of the sensors were detected by the SDFIS. If one or two sensor data does not match any faulty or normal condition, the unmatched sensor likely has a problem. With this method, the SDFIS has ability to diagnose one or two sensors error.

The SDFIS had six MFs for the input and output values, as shown respectively in Fig. 3. SDFIS with one and two sensor errors held twenty-seven rules of inference that were used in reasoning. To detect the sensor errors, there are nine fuzzy rules for the possible errors in the fuzzy rule base. On the other hand, there are eight fuzzy rules for the faulty conditions for the system fault, a fuzzy rule for the normal condition, and nine fuzzy rules for the possible (unknown status) cases.

In this study, the Mamdani-type fuzzy system was employed to map all input variables. For better understanding of input variables, it is necessary to explain the input variable labeled LP as an example. The mapping of the low pressure (LP) to the seven fuzzy values is characterized by membership functions, as shown in Fig. 4. These fuzzy values are very low (VL), low (L), partial low (PL), normal (N), partial high (PH), high (H), and very high (VH).

The FIS contains four major parts: fuzzification, inference engine, fuzzy-rule base, and defuzzification.

Regarding this example (Fig. 4), in the fuzzification process, the membership degree (μ_{LP}) of LP is found which the input variable LP belongs to the fuzzy set of PL. Whereas the value of LP has 0 or 1 in the crisp logic, the value of LP = 204 belongs to the fuzzy set of L to a degree of 0.84 and simultaneously to the fuzzy set of PL to a degree of 0.13.

Fig. 4 also shows how a FIS diagnoses the fault by selecting the fault codes (FAULT-CODES) and the output status (WHY) for the refrigeration system when the values (LP, HP, SH, SC, Mref, and Tsur) are given.

For the output variable, the output fuzzy sets which are activated by the fuzzy rules are then added into a single fuzzy set by using the maximum-operator. The output of the aggregation process is one fuzzy subset for each output variable.

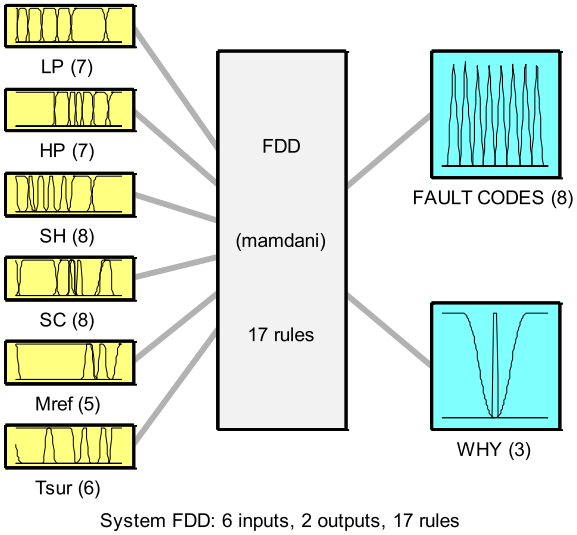

Fig. 3 – Plot out of fuzzy inference system structural characteristics for fault diagnosis of systems. (LP: Low pressure, HP: H pressure, SH: Superheat, SC: Subcooling, Mref: Mass flow rate of refrigerant, Tsur: Surface temperature of computer, FAULTCODES: Fault codes, and WHY: Output status).

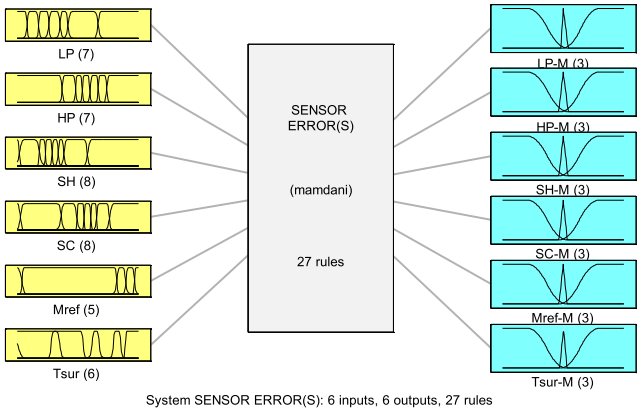

Fig. 4 – Plot out of fuzzy inference system structural characteristics for errors diagnosis of sensors. (LP: Low pressure, HP: High pressure, SH: Superheat, SC: Subcooling, Mref: Mass flow rate of refrigerant, Tsur: Surface temperature of computer, LP-M: Low pressure sensor error, HP-M: High pressure sensor error, SH-M: Superheat sensor error, SC-M: Subcooling sensor error, Mref-M: Mass flow rate sensor error, and Tsur-M: Sensor surface temperature sensor error).

Table 2 – Experimental data.

Measurements / Fault Modes	P_e [kPa]	P_c [kPa]	T_1 [°C]	T_2 [°C]	T_3 [°C]	T_4 [°C]	T_{sur} [°C]	$\dot{m}$ [gs^{-1}]
NC	225	990	10	59	38.3	3.2	38.5	3.9
CDW	560	560	25	25	25	25	25	0
RFD	210	980	14.5	61.5	37.6	1.6	40	3.0
RXV	190	950	16.3	61.2	37.1	−0.2	40.7	2.7
CVL	280	860	10	63.3	34.5	7.6	41.5	2.9
RU	190	860	20.1	62.5	34.1	−0.2	41	2.5
RO	256	1090	6.2	50.5	40.3	5.7	32	2.6
DC	230	1300	17.1	70.4	48.9	3.6	42	3.6
EFF	195	840	0.5	46.5	33.8	0.5	24.4	3.4

Table 3 – The classification of the observed variables.

Measurements	P_e [kPa]		P_c [kPa]		T_{sh} [K]		T_{sc} [K]		$\dot{m}$ [gs^{-1}]		T_{sur} [K]	
Assigned classification	min	max	min	max	min	max	min	max	min	max	min	max
No	–	–	–	–	0	0.1	0	0.1	0	0.1	25	25.1
VL	190	195	560	830	0.1	2	0.1	3.0	0.1	2.5	25.1	30
L	195	200	830	930	2	4	3.0	3.5	2.5	3.0	30	34
PL	200	220	930	980	4	6	3.5	4.0	3.0	3.5	34	38
N	220	230	980	1020	6	8	4.0	4.5	3.5	4.0	38	40
PH	230	250	1020	1100	8	11	4.5	5.5	–	–	40	42
H	250	280	1100	1200	11	15	5.5	6.5	–	–	–	–
VH	280	560	1200	1300	15	21	6.5	7.5	–	–	–	–

All fuzzy sets assigned to each output variable are combined together to form a single fuzzy set for each output variable using a fuzzy aggregation operator.

At the end, a crisp number for the output variable is determined by defuzzification process. The center-of-area method has been used here, so that the crisp output value FAULT-CODES and WHY is the geometrical center of the output fuzzy set.

5. Results and discussion

First, eight faulty scenarios in the basic refrigeration system will be discussed. Second, the use of the p-h diagram for fault detection and diagnosis will be discussed. Third, the classification of the observed variables for applying to FIS and ANN will be discussed. Fourth, the assigned classifications will be applied to FIS and ANN, respectively. Finally, sensor errors will be detected by using FIS.

Table 4 – Symptoms of failure.

Input data / Fault Modes	P_e [kPa]	P_c [kPa]	T_{sh} [K]	T_{sc} [K]	$\dot{m}$ [gs^{-1}]	T_{sur} [K]
NC	N	N	N	N	N	N
CDW	VH	VL	No	No	No	No
RFD	PL	PL	H	PH	L	PH
RXV	VL	PL	VH	N	L	PH
CVL	H	L	L	PL	L	PH
RU	VL	L	VH	VH	VL	PH
RO	H	PH	VL	H	L	L
DC	PH	VH	H	PH	PL	PH
EFF	L	VL	VL	L	PL	VL

The recently proposed diagnostic method for eight faulty scenarios in the basic refrigeration system was based on the refrigeration cycle on the p-h diagram (Kocyigit et al., 2014). We considered using data of this proposed method to diagnose automatically the system faults and the sensor error. According to the previously diagnostic method, we considered recreating the data tables. For this propose, the numbers of the fault code were assigned respectively from 0 to 8 and the name of the fault modes in the same order were assigned for one normal and eight faulty conditions as shown in Table 1. This table also indicates the descriptions of faults and determination of level of fault. Table 2 shows that the each fault mode had a unique data set with respect to the measurements of the thermodynamic properties (Kocyigit et al., 2014).

By using data from Table 2, first the degree of suction superheat (T_{sh}) and the degree of subcooling (T_{sc}) were calculated by using the saturated liquid and vapor data from thermodynamic property table. Then the isentropic efficiency (η_s) was calculated by using Eq. (2). When plotting the p-h diagram by using CoolPack (CoolPack, 2010) software, the evaporating pressure temperature (P_e), the condensing pressure (P_c), T_{sh}, T_{sc}, and η_s were used as input data. Under the normal condition, the refrigeration cycle would stay within normal boundaries by using its unique data set of the normal condition. However, when the system has a faulty condition, the refrigeration cycle would operate out of the normal boundaries. Each faulty condition could be identified from the unique refrigeration cycle. The fault was diagnosed by comparing the normal condition with the faulty conditions. The cycle of normal and faulty conditions were plotted with the dash and continuous lines respectively for comparing the normal cycle with the faulty cycle (Kocyigit et al., 2014).

Table 5 – Average estimation errors with LM, SCG, and RB type ANNs.

Hidden nodes	LM [%]		Hidden nodes	SCG [%]		Hidden nodes	RB [%]	
	Training	Testing		Training	Testing		Training	Testing
6	2.7677	0.8517	34	0.6822	0.32243	4	3.2591	2.0228
7	0.72829	0.67118	35	0.74149	0.35259	5	2.9109	1.8194
8	0.22623	0.15281	36	0.59476	0.33971	6	1.1464	0.7156
9[a]	0.007724	0.00295	37	0.5431	0.36435	7[a]	0.54589	0.40631
10	0.6185	0.057908	38	0.87177	0.30129	8	1.236	0.86645
11	0.62623	0.19257	39[a]	0.44237	0.24916	9	0.74526	0.62244
12	0.13172	0.004128	40	0.56067	0.26321	10	1.3197	0.9488

[a] Best result.

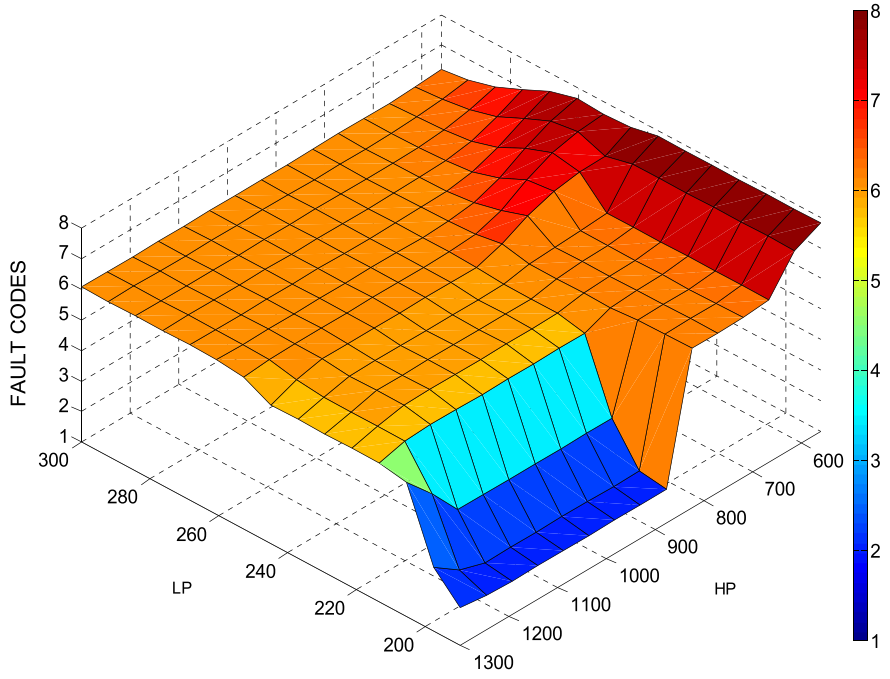

Fig. 5 – FIS plot out of FAULT CODES with respect to LP and HP. (FAULT CODES: Fault codes, LP: Low pressure, and HP: High pressure).

The observed and calculated variables for eight faulty and one normal condition were classified by using their unique data set. A group of symbols was assigned to determine the status of data for each variable as shown in Table 3. According to comparison of data for eight faulty and one normal condition, the minimum–maximum limits of data for each variable were determined as indicated in Table 4. Each faulty condition caused malfunctions in the refrigeration system and could be diagnosed from the symptoms of failures listed in Table 5.

The proposed fault diagnostic FIS for the system faults (FDFIS) was used for the diagnosis of the system faults (Fig. 3). A surface viewer for the FDFIS is shown in Fig. 5. Colors in Fig. 5 show the number of fault code. For better understanding of the proposed fault diagnosis method for the refrigeration system, let us consider the system had a data set of CVL fault. If worn cylinder surfaces and piston rings as well as a clogged valve plate can cause compressor valve leakage (CVL), the simulation of CVL occurs. If the possible fault is CVL, the fault mode of CVL can be diagnosed by the following fuzzy rule:

Rule of CVL:

If low pressure (LP) is HIGH
and high pressure (HP) is LOW
and superheat (SH) is LOW
and subcooling (SC) is LOW
and mass flow rate of refrigerant (Mref) is LOW
and surface temperature of compressor (Tsur) is VERY HIGH
then the selection of FAULT-CODES is CVL and
WHY is TROUBLE

In Rule of CVL, the crisp input values (LP, HP, SH, SC, Mref, and Tsur) are mapped to a degree of membership to the fuzzy values HIGH, LOW, HIGH, LOW, LOW, and VERY HIGH, respectively. While the antecedent of the rule ("if" part) comprises single numbers between 0 and 1, the consequent of the rule ("then" part) assigns the entire inferred fuzzy set to the output variable (FAULT-CODES) and the fuzzy set WHY to the output variable.

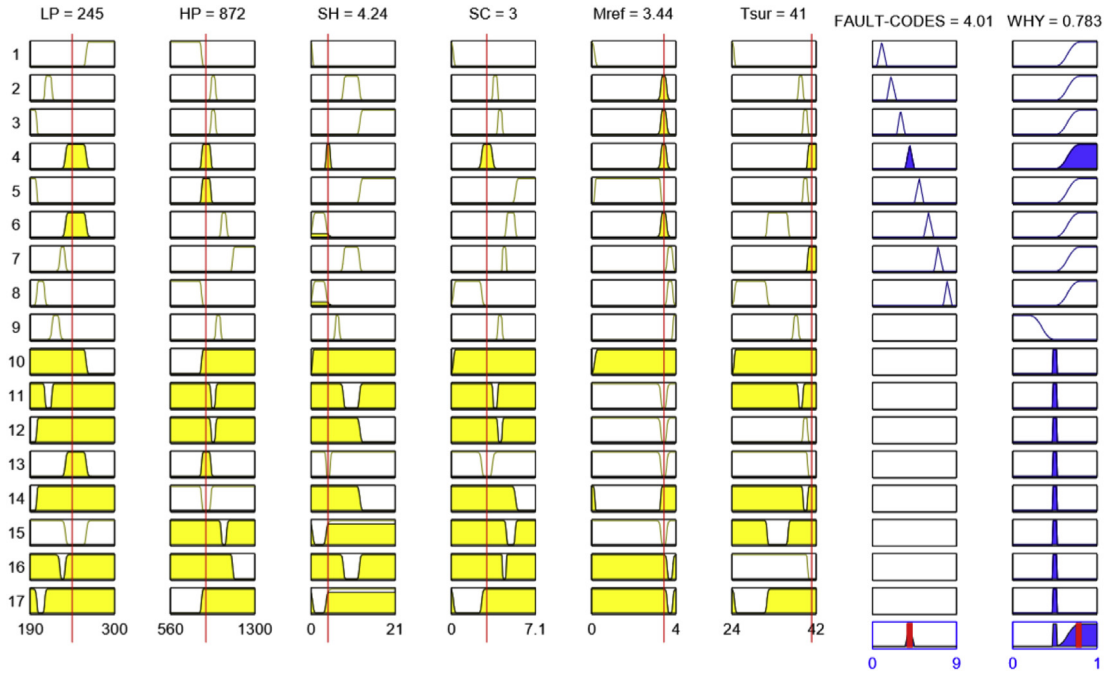

Fig. 6 – The rule view with the fault code 4. (LP: Low pressure, HP: High pressure, SH: Superheat, SC: Subcooling, Mref: Mass flow rate of refrigerant, Tsur: Surface temperature of compressor, FAULT-CODES: Fault codes, and WHY: Output status).

If the possible faults are the statuses of NORMAL and UNKNOWN, they analogously can be diagnosed by the following two fuzzy rules:

Rule of NORMAL:

If low pressure (LP) is NORMAL
or high pressure (HP) is NORMAL
or superheat (SH) is NORMAL
or subcooling (SC) is NORMAL
or mass flow rate of refrigerant (Mref) is NORMAL
or surface temperature of compressor (Tsur) is NORMAL
then the selection of WHY is OK.

Rule of UNKNOWN:

If low pressure (LP) is not VERY LOW
or high pressure (HP) is not PARTIALLY LOW
or superheat (SH) is not VERY HIGH
or subcooling (SC) is not NORMAL
or mass flow rate of refrigerant (Mref) is not LOW
or surface temperature of compressor (Tsur) is HIGH
then the selection of WHY is UNKNOWN.

FDFIS can detect CVL and the rule viewer indicates the fault code 4, as shown in Fig. 6. The fault code 4 means the compressor valve leakage (CVL). When the fault code is slightly over or under the fault codes, it was rounded. Each fault code was tested in the same way. Always the estimations of the FIS were correct. FDFIS can classify the given cases in three categories. These are normal (NC), faulty, and unknown statues.

The proposed sensor error diagnostic FIS (SDFIS) was used for the diagnosis of the error of the sensor (Fig. 4). SDFIS can diagnose one or two sensor errors. Let us consider the system had one sensor error such as the low pressure sensor error (LP-M). In this case, SDFIS detected the error of the LP-M type of the sensor. If the system has two sensor errors, SDFIS detected two sensor errors. Let us consider the system had two sensor errors such as the low pressure sensor error (LP-M)) and the high pressure sensor error (HP-M). LP-M can be detected by the following given fuzzy rule:

Rule of LP-M:

If low pressure (LP) is HIGH
and high pressure (HP) is LOW
and superheat (SH) is LOW
and subcooling (SC) is LOW
and mass flow rate of refrigerant (Mref) is LOW
and surface temperature of compressor (Tsur) is VERY HIGH
then the selection of LP-M is MULFUNCTION and HP-M is OK and SH-M is OK and SC-M is OK and Mref-M is OK and Tsur-M is OK

LP-M and SH-M can be detected by the following given fuzzy rule:

Rule of LP-M and SH-M:

If low pressure (LP) is HIGH
and high pressure (HP) is LOW
and superheat (SH) is LOW
and subcooling (SC) is LOW
and mass flow rate of refrigerant (Mref) is LOW
and surface temperature of compressor (Tsur) is VERY HIGH

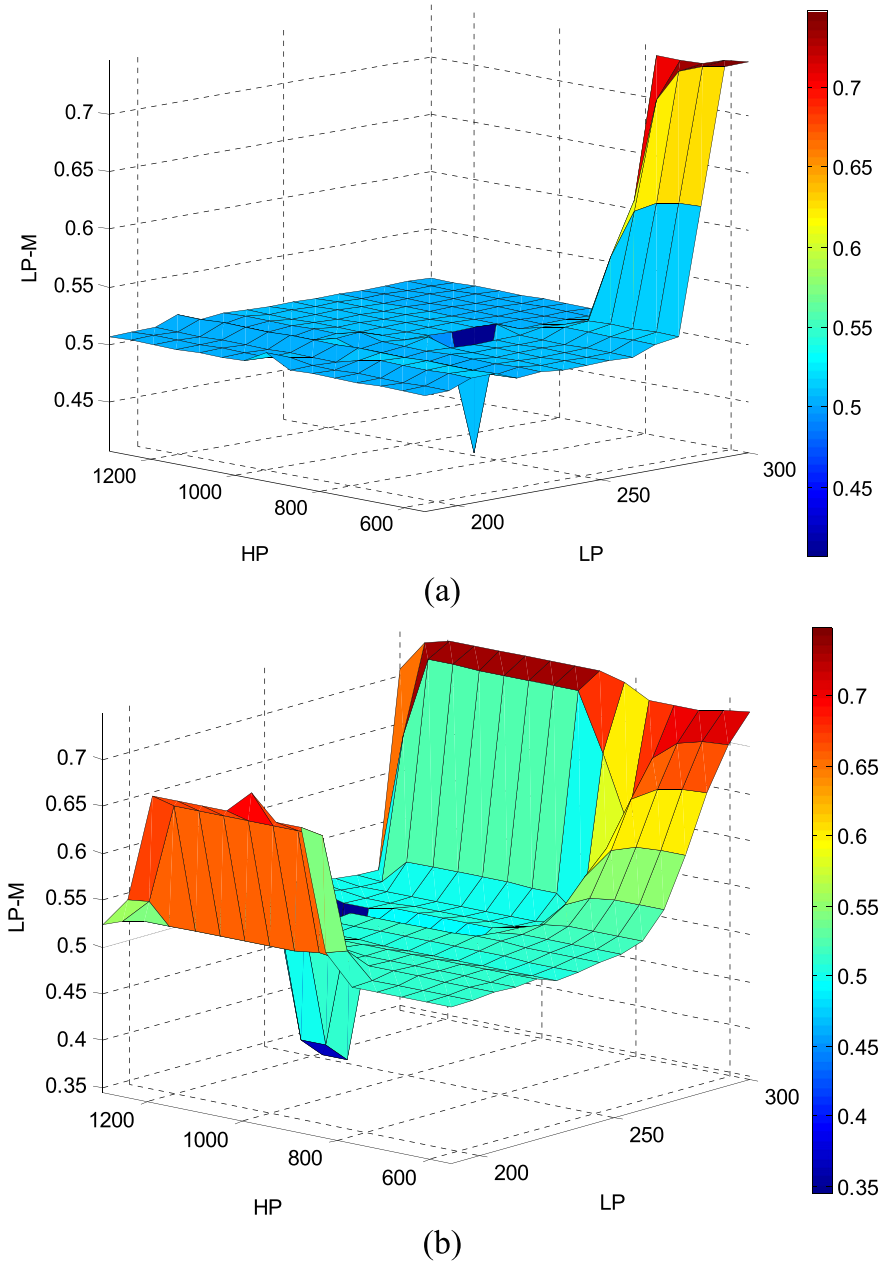

Fig. 7 – Surface view of malfunction of LP-M. (a) Single sensor error for LP sensor (b) Double sensor errors for LP and SH sensors (LP-M: Malfunction of low pressure sensor, LP: Low pressure, and HP: High pressure).

then LP-M is MULFUNCTION and HP-M is OK and SH-M is MULFUNCTION and SC-M is OK and Mref-M is OK and Tsur-M is OK. If (LP is not H)

According to the fuzzy rule base of the single and double sensor errors, two surface viewers for the SDFIS demonstrated the single and double sensor errors, as shown in Fig. 7. Fig. 7(a) demonstrates the single sensor error for LP sensor, while Fig. 7(b) demonstrates the double sensor errors for LP and SH sensors.

To demonstrate the applicability of the ANN to the fault diagnosis of the refrigeration system, eight faulty and one normal condition were also applied to the ANN for the fault detection and diagnosis. Data for the ANN was generated by using the same FDFIS. 66% of data was used for the training case, and the rest of data was used for the testing case. The performance of the ANN was first evaluated by assessing the estimation errors on the training data. Later, the estimation error was calculated one more time after the ANN predicts the output(s) for the 34% of the cases which were not used during the training process. The average percentage error for every predicted output of training and testing data with respect to the range of target data was defined by

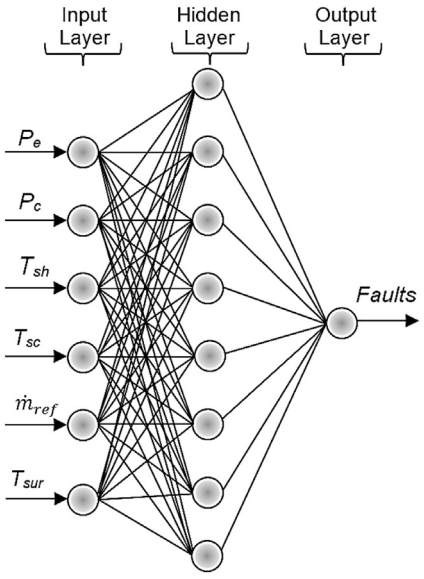

Fig. 8 – Network architecture of ANN model. (Pe: Evaporating pressure, Pc: Condensing pressure, Tsh: Superheat, Tsc: Subcooling, $\dot{m}_{ref}$: Mass flow rate of refrigerant, Tsur: Surface temperature of compressor, and Faults: Fault codes).

$$Er_{ave} = \frac{1}{n}\frac{\sum_{i=0}^{n}|A^e - A^p|}{|A^e_{max} - A^e_{min}|} \quad (3)$$

where A^e is the experimental data, A^p is the predicted result, and n is the number of data.

For ANN application, the Levenberg Marquart (LM), the Scaled Conjugate Gradient (SCG), and the Resilient Backpropagation (RB) algorithms were used to evaluate the inputs and the outputs of data. One input layer, one hidden layer, and one output layer were used for ANN application, as shown in Fig. 8. The use of more than one hidden unit translates to significantly increased test time, which is more valuable than training time in practice (Yu and Deng, 2012). The evaluation of the performance of ANNs was applied between 1 and 40 nodes to LM, SCG, and RB. The scenarios of all faulty and one normal condition were trained to estimate the faulty condition by using ANN. According to Table 5, the best estimations were obtained when the hidden nodes were selected 9, 39, and 7 with the LM, SCG, and RB type ANN were used respectively. For compact representation and consistency, the LM type ANN with 9 nodes was selected. The R_{ave} value for the LM was 0.007724%.

According to generated data and predicted data, all faulty and one normal condition for fault diagnosis with LM were shown in Fig. 9. This Fig. 9 also shows the testing results of the faulty and one normal condition for fault diagnosis with LM. The average errors of LM, SCG, and RB during the testing process were indicated in Fig. 10.

6. Conclusions

The author previously estimated eight faulty conditions by observing variables of the thermodynamic properties and the refrigeration cycle on the p-h diagram. In this study, a diagnostic fuzzy inference system and an artificial neural network were developed to diagnose faults in a vapor compression refrigeration experimental setup by using eight faulty conditions and one normal condition. In addition, a different set of fuzzy inference system was also developed to diagnosis sensor errors on the experimental setup. A fault diagnostic fuzzy inference system for system faults and an error diagnostic fuzzy inference system for sensor errors, and three types of artificial neural networks were tested by using six

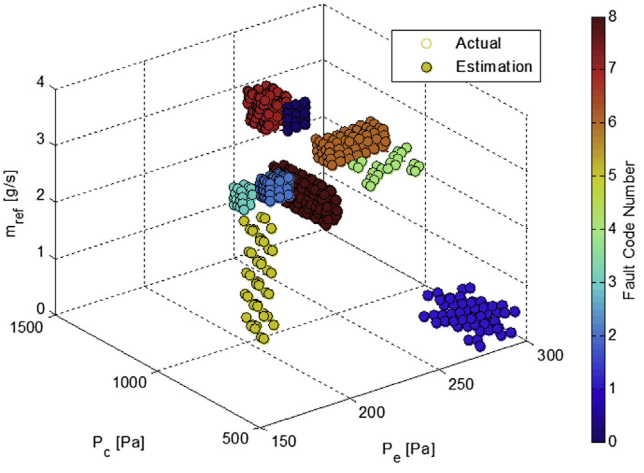

Fig. 9 – The plot out of fault code number with respect to Pe, Pc, and $\dot{m}_{ref}$ for fault diagnosis with LM. (Pe: Evaporating pressure, Pc: Condensing pressure, and $\dot{m}_{ref}$: Mass flow rate of refrigerant).

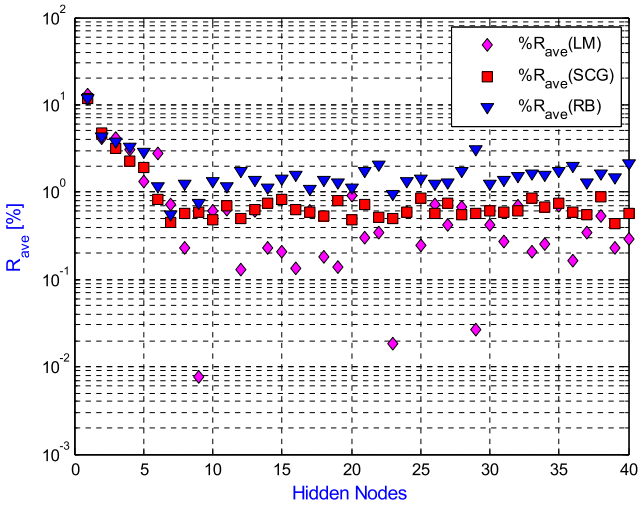

Fig. 10 – Estimating errors (%Rave) during the testing process for fault diagnosis with LM, SCG, and RB. (%Rave: Percentage error in the range of estimate data, LM: Levenberg-Marquart, SCG: Scaled conjugate gradient backpropagation, and RB: Resilient backpropagation).

sensor data. For this purpose, eight common fault scenarios and one normal condition were applied to the FIS and a Levenberg Marquart (LM), a Scaled Conjugate Gradient (SCG), and a Resilient Backpropagation (RB) types neural networks were used to train and test eight faulty conditions, and results have been discussed in terms of possible faults in basic refrigeration systems and sensor errors. The LM type ANNs provided the minimum estimation errors.

Performance of the tested systems verified that the proposed fault diagnostic FIS and the ANN had an ability to diagnose eight faults in the basic refrigeration system. Moreover the proposed error prognostic fuzzy inference system had also ability to detect error of one or two sensors.

The FIS and ANN based diagnostic systems effectively detected the problems and classified the faults in the study. These approaches eliminated the need of extensive modeling for the use of analytic models.

REFERENCES

Abraham, A., 2005. Rule-based expert systems. In: Sydenham, P.H., Thorn, R. (Eds.), Handbook of Measuring System Design. John Wiley & Sons, Ltd. Article 130.

Bulgurcu, H., 2009. Maintenance, Troubleshooting and Service Process in HVAC&R Systems. In: ISKAV Technical Book Series No: 5. Istanbul (printed in Turkish).

CoolPack, 2010. A Collection of Simulation Tools for Refrigeration. Available at: Url: www.et.dtu.dk/CoolPack (accessed 16.06.13.).

Ertunc, H.M., Hosoz, M., 2008. Comparative analysis of an evaporative condenser using artificial neural network and adaptive neuro-fuzzy inference system. Int. J. Refrigeration 31, 1426–1436.

Halm-Owoo, A.K., Suen, K.O., 2002. Applications of fault detection and diagnostic techniques for refrigeration and air conditioning: a review of basic principles. Proc. Inst. Mech. Eng. Part E: J. Process Mech. Eng. 216, 121–132.

Han, H., Gu, B., Wang, T., Li, Z.R., 2011. Important sensors for chiller fault detection and diagnosis (FDD) from the perspective of feature selection and machine learning. Int. J. Refrigeration 34, 586–599.

Hou, Z., Lian, Z., Yao, Y., Yuan, X., 2006. Data mining based sensor fault diagnosis and validation for building air conditioning system. Energy Convers. Manag. 47, 2479–2490.

Kim, M., Yoon, S.H., Domanski, P.A., Payne, W.V., 2008. Design of a steady-state detector for fault detection and diagnosis of a residential air conditioner. Int. J. Refrigeration 31, 790–799.

Kim, M., Yoon, S.H., Payne, W.V., Domanski, P.A., 2010. Development of the reference model for a residential heat pump system for cooling mode fault detection and diagnosis. J. Mech. Sci. Technol. 24 (7), 1481–1489.

Kizilkan, O., 2011. Thermodynamic analysis of variable speed refrigeration system using artificial neural networks. Expert Syst. Appl. 38, 11686–11692.

Kocyigit, N., Bulgurcu, H., Lin, C., 2014. Fault diagnosis of a vapor compression refrigeration system with hermetic reciprocating compressor based on p-h diagram. Int. J. Refrigeration 4 (5), 4 4–5 4.

Mavromatidis, G., Acha, S., Nilay, S., 2013. Diagnostic tools of energy performance for supermarkets using artificial neural network algorithms. Energy Build. 62, 304–314.

Piacentino, A., Talamo, M., 2013. Innovative thermoeconomic diagnosis of multiple faults in air conditioning units: methodological improvements and increased reliability of results. Int. J. Refrigeration 36, 2343–2365.

Wang, S.K., 2001. Handbook of Air Conditioning and Refrigeration, second ed. McGraw-Hill, New York. Available at: Url: http://www.gmpua.com/CleanRoom/HVAC/Cooling/HandbookofAirConditioningandRefrigeration.pdf. (accessed 30.12.13.).

Yan, K., Shen, W., Mulumba, T., Afshari, A., 2014. ARX model based fault detection and diagnosis for chillers using support vector machines. Energy Build. 81, 287–295.

Yoon, S.H., Payne, E.V., Domanski, P.A., 2011. Residential heat pump heating performance with single faults imposed. Appl. Therm. Eng. 31, 765–771.

Yu, D., Deng, L., 2012. Efficient and effective algorithms for training single-hidden-layer neural networks. Pattern Recognit. Lett. 33, 554–558.

Zhao, X., Yang, M., Li, H., 2012. A virtual condenser fouling sensor for chillers. Energy Build. 52, 68–76.

Zhao, X., Yang, M., Li, H., 2014. Field implementation and evaluation of a decoupling-based fault detection and diagnostic method for chillers. Energy Build. 72, 419–430.

Zhu, Y., Jin, X., Du, Z., 2012. Fault diagnosis for sensors in air handling unit based on neural network pre-processed by wavelet and fractal. Energy Build. 44, 7–16.